

Electronic states of impurity atoms in noble-metal lattices

Martin J. G. Lee

Department of Physics and Scarborough College, University of Toronto, Toronto, Canada M5S 1A7

N. A. W. Holzwarth*

Department of Physics, University of Toronto, Toronto, Canada M5S 1A7

P. T. Coleridge

Division of Physics, National Research Council of Canada, Ottawa, Canada K1A 0R6

(Received 13 October 1975)

Experimental Dingle-temperature anisotropies and impurity-induced Fermi-surface changes in nonmagnetic dilute alloys have been shown elsewhere to determine the Friedel phase shifts that characterize impurity scattering. In the present paper the Friedel phase shifts for various dilute alloys in noble-metal hosts are analyzed to yield the complex renormalization coefficients that describe the way in which backscattering modifies the wave-function amplitude on the impurity site, and the phase shifts that characterize potential scattering of conduction electrons at the Fermi level by the impurity. Our approach is based on an exact treatment of backscattering in a lattice of muffin-tin potentials. The influence of possible lattice distortion associated with alloying on the determination of the impurity-state parameters is discussed. Impurity-state parameters are obtained for dilute noble-metal alloys which give information about the scattering potentials and, in some cases, charge shifts associated with alloying can be inferred. Various approximate treatments of backscattering are developed, which generally work well except in the vicinity of scattering resonances of the host or impurity atom.

I. INTRODUCTION

Of the various experimental techniques which have been developed to explore metallic properties that depend on the impurity-induced scattering of conduction electrons in dilute alloys,¹ those that are most fully developed at the present time are de Haas-van Alphen measurements of the anisotropy of that component of the Dingle temperature which is proportional to the concentration of impurities,¹ and of concentration-dependent changes in de Haas-van Alphen frequency. Such measurements promise to yield detailed information about the T matrix which describes the scattering of conduction electrons between states on the Fermi surface. Inversion techniques have been developed to combine Dingle-temperature data for many intersecting orbits to determine the relaxation time at each point on the Fermi surface,²⁻⁴ and steps have been taken towards relating the data to the anisotropy of scattering of conduction electrons.⁵⁻⁹ The corresponding experimental studies of Fermi-wave-vector anisotropies in dilute alloys are also possible,¹⁰ and it appears that these can be interpreted in a similar fashion.¹¹ In other experiments the electronic charge density in the vicinity of the impurity atoms has been determined from high-resolution studies of host Knight shifts,¹² and studies of concentration-dependent spin relaxation for heavy-metal impurities promise to provide a measure of spin-orbit interaction on the impurity site.¹³

The T matrix at each point on the Fermi sur-

face depends on the host-metal wave function at that point. The host wave functions can be determined by phase-shift analysis of experimental cross sectional areas of the Fermi surface carried out, for example, by the band-structure method of Korringa, Kohn, and Rostoker¹⁴ (KKR). If the symmetry character of the host wave functions varies (from predominantly s -like to p -like or d -like) over the Fermi surface, the impurity-induced anisotropies measured by the de Haas-van Alphen experiments on dilute alloys can be interpreted to yield a set of scattering parameters. It is convenient to choose as scattering parameters the set of Friedel phase shifts¹⁵ that characterizes scattering by a single substitutional impurity in an ideal lattice of muffin-tin potentials, because these have the property of being essentially independent of the muffin-tin zero. A practical complication is that the Friedel phase shifts determined from analysis of experimental data will also contain a contribution from any lattice distortion caused by the impurity, which is not the same for the two types of experiments.

In a recent paper Coleridge, Holzwarth, and Lee,¹⁵ have carried out a nonrelativistic analysis of Dingle-temperature data for several nonmagnetic dilute alloys in noble-metal hosts, in order to determine the Friedel phase shifts associated with impurity scattering. The Friedel phase shifts depend on the scattering potential of the impurity and on back scattering by the host lattice. The purpose of the present paper is to explore the separation of the Friedel phase shifts into impuri-

ty-scattering and host back scattering terms. We shall show that it is inconsistent to analyze impurity-scattering data while neglecting back scattering. We shall adopt two distinct treatments of back scattering. The first is based on a recent calculation by Holzwarth of the scattered wave in the vicinity of a single impurity atom in a lattice of muffin-tin potentials.¹⁶ This calculation leads to a treatment of back scattering which is exact in the muffin-tin approximation. An alternative approach which involves less computation will be described, based on a series of approximations similar to the "minimum scattering approximation" described briefly elsewhere.¹⁷ These simple approximations to back scattering are expected to work best in nearly-free-electron hosts; in the noble metals it is advantageous to carry out the exact calculation.

The outline of this paper is as follows. In Sec. II we review the treatment of host-lattice effects in impurity scattering. In Sec. III we outline the method used for the exact nonrelativistic calculations of the back scattering coefficients and discuss the various approximations that can be made for these coefficients.

II. HOST-LATTICE EFFECTS IN IMPURITY SCATTERING

Assuming incoherent scattering by an atomic fraction c of impurities, the inverse relaxation time association with a Bloch state of wave vector \vec{k} on the Fermi surface is given by the Fermi-surface integral

$$\frac{1}{\tau(\vec{k})} = \frac{2\pi c}{\hbar} \frac{\Omega}{(2\pi)^3} \int \frac{|T_{\vec{k}\vec{k}'}|^2 dS_{\vec{k}'}}{\hbar V_{\vec{k}'}} , \quad (1)$$

where Ω is the volume of the unit cell and $V_{\vec{k}'}$ is the velocity of the state \vec{k}' . The transition matrix must also satisfy the optical theorem, which expresses the physical constraint of conservation of flux in the scattering process

$$\frac{\Omega}{(2\pi)^3} \int \frac{|T_{\vec{k}\vec{k}'}| dS_{\vec{k}'}}{\hbar V_{\vec{k}'}} = -\frac{\text{Im} T_{\vec{k}\vec{k}}}{\pi} . \quad (2)$$

So the inverse relaxation time at a point on the Fermi surface is simply related to the imaginary part of the diagonal element of T at that point¹⁷

$$1/\tau(\vec{k}) = -(2c/\hbar) \text{Im} T_{\vec{k}\vec{k}} . \quad (3)$$

In the simplest model of the scattering of conduction electrons by impurity atoms, the host metal is treated in the free-electron approximation. It follows then that $\text{Im} T_{\vec{k}\vec{k}}$ and $1/\tau(\vec{k})$ are isotropic, so the model cannot account for the experimentally observed anisotropies of $\tau(\vec{k})$ and it is of course impossible to determine the scattering phase shifts.

Morgan⁵ generalized the T -matrix formulation to describe scattering between Bloch states in a lattice of muffin-tin potentials. He pointed out that the primary outgoing spherical wave produced by im-

purity scattering, which can be expanded in the form

$$b_{1m} h_1(\kappa\rho) Y_{1m}(\theta, \phi) , \quad (4)$$

is to some extent back scattered by the host lattice. To describe this effect he introduced a back scattering matrix $T_{1m,1'm'}$, in terms of which the back scattered wave can be written

$$b_{1m} \sum_{1'm'} T_{1m1'm'} j_{1'}(\kappa\rho) Y_{1'm'}(\theta, \phi) . \quad (5)$$

(In these formulas j_l and h_l are spherical Bessel and Hankel functions and Y_{lm} are spherical harmonics.) The effect of back scattering is to renormalize the Bloch wave amplitude inside the impurity cell. Morgan arrived at a generalized transition matrix, whose elements take the form

$$\begin{aligned} T_{\vec{k}\vec{k}'}(E) = & -\frac{\hbar^2}{2m\kappa} \sum_{1m} a_{1m}^*(\vec{k}, E) a_{1m}(\vec{k}, E) \\ & \times \left[1 + \left(\sum_{1'm'} T_{1m1'm'} b_{1'm'} \right) / a_{1m}(\vec{k}, E) \right] \\ & \times \sin\Delta\eta_1 \exp(i\Delta\eta_1) , \end{aligned} \quad (6)$$

where $\Delta\eta_1 \equiv \eta_1^i - \eta_1^f$ denotes the phase-shift difference between the impurity and host atom at the Fermi energy of the host metal, and where the Bloch coefficients $a_{1m}(\vec{k})$ can be calculated from the zero eigenvector of the KKR secular matrix for the host lattice.

Blaker and Harris⁶ simplified the muffin-tin treatment of impurity scattering by expanding the partial waves in a series of cubic harmonics. For a cubic environment they showed that the renormalization factors, $(1 + \sum T b/a)$ in Morgan's notation, are complex, energy-dependent coefficients that are, however, independent of the wave vector \vec{k} . The renormalization factors can therefore be written as $\alpha_L(E)$, where L is an abbreviated notation for the distinct representations of the cubic point group ($L \equiv l, \Gamma$). The importance of Blaker and Harris's result is that experimental scattering anisotropies, such as anisotropic Dingle temperature data, can be analyzed to yield the value of the scattering parameter

$$\text{Im}[\alpha_L(E_F) \sin\Delta\eta_1 \exp(i\Delta\eta_1)] \quad (7)$$

associated with each partial wave. Nonrelativistic parametrizations of experimental Dingle temperature anisotropies for noble-metal alloys have been carried out by Coleridge,⁷ by Harris and Mulimani,⁹ and by Brown and Myers,³ including all partial waves up to $l=2$, but in these calculations only the scattering parameters were deduced; it was not possible to deduce the scattering phase shifts because the back scattering coefficients α_L were unknown.

Holzwarth¹⁶ showed that in general a single substitutional impurity in a muffin-tin lattice causes

mixing between the various partial waves. In cubic lattices having one atom per primitive unit cell, such as the alkali and noble metals, the general form of the T matrix that describes scattering from a Bloch state \vec{k} to \vec{k}' is

$$T_{\vec{k}\vec{k}'}(E) = -\frac{\hbar^2}{2m\kappa} \sum_{\Gamma\gamma} a_{\Gamma\gamma}^*(\vec{k}', E) a_{\Gamma\gamma}(\vec{k}, E) \times \alpha_{\Gamma}^{\Gamma}(E) \sin\Delta\eta_{\Gamma} \exp(i\Delta\eta_{\Gamma}), \quad (8)$$

where Γ denotes an irreducible representation of the cubic group, and γ denotes a particular member of that representation. The matrix $\alpha_{\Gamma}^{\Gamma}(E)$, termed the renormalization matrix, describes the effects of back scattering of the primary spherical scattered wave by the host lattice. However, the renormalization matrix $\alpha_{\Gamma}^{\Gamma}(E)$ has no elements between different representations of the cubic group so off-diagonal elements occur only between values of l having one or more representations in common. Those irreducible representations of the cubic group which correspond to small values of l are given in Table I. We note that an important simplification arises in a nonrelativistic analysis for $l \leq 2$, for each representation of the cubic group is then associated with a different angular momentum state (see Table I), and the renormalization matrix is diagonal:

$$\alpha_{\Gamma}^{\Gamma} = \alpha_L \delta_{\Gamma\Gamma}. \quad (9)$$

In this case the renormalized impurity amplitude is proportional to the corresponding Bloch wave amplitude, the constants of proportionality being the four complex renormalization coefficients $\alpha_L(E)$. Holzwarth's expression for the T matrix then reduces to the form given by Blaker and Harris

$$T_{\vec{k}\vec{k}'}(E) = \frac{-\hbar^2}{2m\kappa} \sum_{L\gamma} a_{L\gamma}^*(\vec{k}', E) a_{L\gamma}(\vec{k}, E) \times \alpha_L(E) \sin\Delta\eta_L \exp(i\Delta\eta_L). \quad (10)$$

Alternatively, back scattering can be described by Morgan's back scattering matrix, which in cubic harmonic notation can be written $T_{\Gamma}^{\Gamma}(E)$, and which is related to $\alpha_{\Gamma}^{\Gamma}(E)$ by the equation

$$i^{l-l'} \alpha_{\Gamma}^{\Gamma} = \{ [I - iT^{\Gamma} \sin\eta_{\Gamma}^l \exp(i\eta_{\Gamma}^l)]^{-1} \times [1 - iT^{\Gamma} \sin\eta_{\Gamma}^{l'} \exp(i\eta_{\Gamma}^{l'})] \}_{\Gamma\Gamma}. \quad (11)$$

When the renormalization matrix is diagonal the back scattering matrix is also diagonal so we can define back scattering coefficients T_L by

$$T_{\Gamma}^{\Gamma} = T_L \delta_{\Gamma\Gamma}. \quad (12)$$

The relationship between the renormalization coefficients and the back scattering coefficients then becomes

$$\alpha_L = \frac{1 - iT_L \sin\eta_L^l \exp(i\eta_L^l)}{1 - iT_L \sin\eta_L^{l'} \exp(i\eta_L^{l'})}. \quad (13)$$

The α_L depart from the unity to the extent that the wave function on the impurity site is modified by back scattering by the host lattice. In the limit where the host is free-electron-like $\alpha_L = 1$, so $T_L = 0$, and the back scattered wave vanishes.

In the present paper, concerning the analysis of impurity scattering in noble-metal hosts, we shall consistently neglect scattering into f and higher partial waves, so the simplifications expressed by Eqs. (9) and (12) apply. Then the scattering rate at a point \vec{k} on the Fermi surface is given by Eq. (3), where $\text{Im}T_{\vec{k}\vec{k}}(E_F)$ is to be calculated from Eq. (10). It is convenient to define a set of partial scattering coefficients

$$t_{\vec{k}}^L \equiv \frac{\hbar^2}{2m\kappa} \sum_{\gamma} |a_{L\gamma}(\vec{k}, E)|^2 \quad (14)$$

which depend on the Bloch coefficients of the host wave functions, and a set of scattering parameters

$$S_L \equiv \alpha_L \sin\Delta\eta_L \exp(i\Delta\eta_L) \quad (15)$$

which depend on the impurity potential and on back scattering by the host lattice. In terms of the partial scattering coefficients, the scattering rate at a point on the Fermi surface can be expressed in the form

$$\frac{1}{\tau(\vec{k})} = \frac{2c}{\hbar} \sum_L (\text{Im}S_L) t_{\vec{k}}^L. \quad (16)$$

The scattering parameters $\text{Im}S_L(E_F)$ characterize the impurity scattering of conduction electrons on the Fermi surface. They take into account both the scattering phase shifts of the impurity atoms and the back scattering effects due to the host lattice. It is convenient to write the renormalization coefficients in the form

$$\alpha_L = |\alpha_L| \exp(i\theta_L), \quad (17)$$

so that Eq. (14) becomes

$$S_L = |\alpha_L| \sin\Delta\eta_L \exp(i\phi_L), \quad (18)$$

where effective ("Friedel") phase shifts have been defined by

TABLE I. Irreducible representations of the cubic group associated with spherical harmonics of low angular momentum l .

l				
0	Γ_1			
1	Γ_{15}			
2	Γ_{12}	Γ_{25^*}		
3	Γ_{2^*}	Γ_{15}	Γ_{25}	
4	Γ_1	Γ_{12}	Γ_{15}	Γ_{25^*}

$$\phi_L \equiv \Delta\eta_l + \theta_L . \quad (19)$$

The Friedel phase shifts are so named because they satisfy a sum rule of the form introduced by Friedel¹⁸ for the free-electron gas:

$$\mathfrak{F} \equiv \frac{2}{\pi} \sum_L n(L) \phi_L(E_F) = \Delta Z , \quad (20)$$

where $n(L)$ is the degeneracy of the representation L and ΔZ is the valence difference between host and impurity atoms.¹⁶ By use of the optical theorem, Eq. (2), the scattering parameters S_L can be expressed in terms of the Friedel phase shifts. The result is

$$I_L S_L = \sin\phi_L \exp(i\phi_L) , \quad (21)$$

where the real positive constant I_L is a Fermi surface average of the partial scattering coefficients defined by

$$I_L(E) = \frac{1}{n(L)} \frac{\Omega}{8\pi^2} \int \frac{t_{\mathbf{k}}^L dS_{\mathbf{k}}}{\hbar V_{\mathbf{k}}} . \quad (22)$$

An equivalent analysis involving the real part of S_L has been discussed by Coleridge.¹¹ In the limit where the impurity concentration is sufficiently low that the Fermi energy is unaltered by alloying,^{18,19} the real parts of the scattering parameters give the change in Fermi-surface dimensions. Corresponding to Eq. (19) for the relaxation time, the impurity-induced change in the k vector at the Fermi surface is given by

$$\Delta \vec{k} = \frac{c}{\hbar V_{\mathbf{k}}} \sum_L (\text{Re} S_L) t_{\mathbf{k}}^L . \quad (23)$$

Thus impurity-induced changes in the Fermi-surface dimensions and the relaxation times can be interpreted to yield complementary information about impurity scattering. In practice the partial scattering coefficients $t_{\mathbf{k}}^L$ and the constants I_L are determined from the results of phase-shift analysis of the experimental Fermi-surface anisotropies of the host metals,¹⁵ and the appropriate scattering parameters, $\text{Im}(S_L)$ or $\text{Re}(S_L)$, are then adjusted to fit the experimental data.^{11,15} The magnitudes of the Friedel phase shifts are determined from the scattering parameters and the constants I_L using Eq. (21). Analyzing the Dingle temperature experiments, the otherwise undetermined signs of the Friedel phase shifts are chosen so that the calculated residual resistivities agree with experiment. In several earlier papers, and in parts of the present paper, the distinction between the two d -like representations Γ_{12} and $\Gamma_{25'}$ is ignored. The conditions under which this approximation is satisfactory are discussed below.

We would emphasize that it is inconsistent to analyze de Haas-van Alphen frequency and Dingle-temperature data to determine impurity phase

shifts without allowing for back scattering. This can be demonstrated by combining Eqs. (18) and (21) to eliminate S_L . The result is

$$\sin\phi_L = I_L |\alpha_L| \sin\Delta\eta_l . \quad (24)$$

In the absence of back scattering $\phi_L = \Delta\eta_l$ and $|\alpha_L| = 1$. This is consistent with Eq. (24) only if $I_L = 1$ for all L . However, a partial wave analysis depends on the anisotropy of the partial scattering coefficients $t_{\mathbf{k}}^L$. This means that the integrals I_L defined by Eq. (22) generally depart significantly from unity (even if one of the I_L 's is fortuitously equal to unity this will not normally be true of the other I_L 's). Hence back scattering is negligible only in the limit of a free-electron host, and in that limit the impurity scattering is isotropic.

III. NONRELATIVISTIC TREATMENT OF BACK SCATTERING

A. Exact calculation of coefficients

Exact expressions for the nonrelativistic back scattering coefficients for impurity scattering in cubic host lattices, treating the host and impurity atoms in the muffin-tin approximation, have recently been obtained by Holzwarth.¹⁶ The scattered wave in the vicinity of a substitutional impurity in an otherwise perfect lattice of muffin-tin potentials was calculated by an extension of the Green's-function method of band-structure calculation, following an approach developed by Dupree.²⁰

The scattered wave in the vicinity of the impurity can be expressed in terms of a complex matrix $\chi_{LL'}(E)$, whose elements are those of the Brillouin-zone integral

$$\chi_{L\gamma L'\gamma'}(E) = \frac{\Omega}{(2\pi)^3} \int_{\text{BZ}} d^3k [M^{-1}(\vec{k}, E)]_{L\gamma, L'\gamma'} \quad (25)$$

of the inverse of the KKR secular matrix¹⁶

$$M_{L\gamma L'\gamma'}(\vec{k}, E) = \cot\eta_l^{\delta} \delta_{LL'} \delta_{\gamma\gamma'} + \kappa^{-1} A_{L\gamma, L'\gamma'}(\vec{k}, E) . \quad (26)$$

The integrand is singular on the surface of constant energy $E(\vec{k}) = E$, and so the integral can be expressed as a sum of surface and volume terms. The χ matrix takes the form

$$\begin{aligned} \chi_{L\gamma, L'\gamma'}(E) = & \frac{\Omega}{(2\pi)^3} \mathcal{P} \int_{\text{BZ}} d^3k [M^{-1}(\vec{k}, E)]_{L\gamma, L'\gamma'} \\ & + \frac{i\Omega\hbar^2}{16\pi^2 m \kappa} \sin\eta_l^{\delta} \sin\eta_l^{\delta} \\ & \times \int \frac{dS_{\mathbf{k}} a_{L\gamma}^*(\vec{k}, E) a_{L'\gamma'}(\vec{k}, E)}{|\nabla_{\mathbf{k}} E(\vec{k})|} , \quad (27) \end{aligned}$$

where \mathcal{P} denotes a principal part integral,²¹ and where the surface integral is taken over the surface of constant energy $E(\vec{k}) = E$. Since the principal part integral is over the entire Brillouin zone, only those linear combinations of matrix elements contribute to the result which transform according

to the full point-group symmetry of the lattice. There are therefore no elements of the matrix linking different irreducible representations of the cubic group, or linking different members of a given representation. It is convenient to introduce the abbreviated notation

$$\chi_{L\gamma L'\gamma'}(E) \equiv \chi_{l l'}^\Gamma(E) \delta_{\Gamma\Gamma'} \delta_{\gamma\gamma'} . \quad (28)$$

With the assumption that for $l \geq 3$ the phase-shift differences are negligible, the matrix $\chi_{l l'}^\Gamma(E)$ assumes diagonal form with elements $\chi_L(E)$. In this case, Eq. (30) leads to the following useful identity:

$$\text{Im}\chi_L = I_L \sin^2 \eta_i^h , \quad (29)$$

where I_L was defined by Eq. (25). Our numerical evaluation for the χ coefficients will be described in detail below. Expressed in terms of the χ coefficients, the back scattering coefficients take the form

$$T_L(E_F) = i \{ \chi_L(E_F)^{-1} - [\sin \eta_i^h \exp(i\eta_i^h)]^{-1} \} , \quad (30)$$

while the renormalization coefficients are found from Eqs. (13) and (30) to be

$$\alpha_L(E_F) = \frac{\exp(-i\Delta\eta_i) \sin^2 \eta_i^h}{\sin \eta_i^h \sin \eta_i^i - \sin \Delta\eta_i \chi_L(E_F)} , \quad (31)$$

and it is readily verified that the optical theorem is satisfied.

The evaluation of the χ coefficients for noble-metal lattices was carried out numerically. It is evident from Eqs. (26) and (27) that the effect of the host potential enters the expression for the χ coefficients only in terms of phase shifts evaluated at the Fermi energy of the host lattice. The phase shifts were obtained, as in Ref. 15, by analysis of experimental Fermi-surface anisotropies. This is preferable to first-principles calculation because no crystal potential for the noble metals has yet been constructed which reproduces the Fermi-surface anisotropies to the accuracy with which they are known from experiment.

The Fermi surfaces of the noble metals lie within the first Brillouin zone, and have necks in the eight $\langle 111 \rangle$ directions. The integrals over an irreducible $\frac{1}{48}$ th sector of the Brillouin zone were evaluated, and the Brillouin-zone integrals were obtained by carrying out the appropriate rotations.¹⁶ The volume and surface integrals were performed using a spherical coordinate system having its polar axis along the $\langle 111 \rangle$ direction, except within a region enclosing the neck, defined by a circular frustrum with base in the (111) plane. In both regions, the singular contributions to the Brillouin-zone integral were treated primarily in the radial integration. The principal-part contributions to the radial integral were evaluated by making a Taylor-series expansion of the integrand about the Fermi radius. In the neck region, an additional singular

contribution occurs in the axial integral where the circular frustrum intersects the Fermi surface. The corresponding principal-part contribution was evaluated by removing the singularity from the axial integral and adding the appropriate analytic correction to the final result. All nonsingular integrals were evaluated by Gaussian quadrature. The Fermi radius was iterated until the zero eigenvalue of the secular matrix satisfied $|\lambda(\vec{k}, \epsilon_F)| < 10^{-5}$. Approximately 120 points were used to evaluate the surface contribution to the integral, and approximately 2800 for the volume contribution. Consequently, the Brillouin integral results are expected to be accurate to better than 0.1%. The numerical results for the nonrelativistic χ and T coefficients at the chosen Fermi energies of noble-metal lattices are presented in Table II. Lasseter and Soven²² have evaluated Brillouin-zone integrals equivalent to $\chi_L(E)$ for Cu in connection with a calculation of the impurity-induced change in the density of states. In that work the surface integrals were performed explicitly and the volume contributions were determined from the Kramers-Kronig relations, but their results are not expressed in a form which permits direct comparison with the present work.

B. Analysis of data

Knowing the χ coefficients at the Fermi energy, it is not difficult to fit the experimental Dingle-temperature anisotropies. The scattering parameters, defined by

$$\text{Im}S_L = \text{Im}[\alpha_L(E_F) \sin \Delta\eta_i \exp(i\Delta\eta_i)] , \quad (32)$$

can be written, using Eq. (31), in the form

$$\text{Im}S_L = \sin^2 \eta_i^h \frac{\text{Im}\chi_L}{(\xi - \text{Re}\chi_L)^2 + (\text{Im}\chi_L)^2} , \quad (33)$$

where ξ_i is defined by

$$\xi_i = (\cot \eta_i^h - \cot \eta_i^i)^{-1} . \quad (34)$$

The d -wave contribution to the relaxation time can be written

$$1/\tau_d(\vec{k}) = (2c/\hbar) (t_{\vec{k}}^{\Gamma 12} \text{Im}S_{\Gamma 12} + t_{\vec{k}}^{\Gamma 25'} \text{Im}S_{\Gamma 25'}) , \quad (35)$$

where $\text{Im}S_{\Gamma 12}$ and $\text{Im}S_{\Gamma 25'}$ can be expressed in terms of the single parameter ξ_2 , which is determined by fitting the experimental data. Whereas the s -wave and p -wave fitting parameters $\text{Im}S_0$ and $\text{Im}S_1$ enter the expression for the inverse relaxation time as linear coefficients, the d -wave parameter ξ_2 does not, so a suitable minimization procedure must be developed to make a least-squares fit to the experimental data while maintaining the distinction between the two d -like representations. The scattering parameters for various dilute alloys in noble-metal hosts presented in Table III were obtained by fitting the experimental Dingle-temperature

TABLE II. Nonrelativistic band-structure and back scattering parameters for the noble metals.

Host	$l \Gamma$	η_i^h	I_L	$\text{Re}\chi_L$	$\text{Im}S_L$	$\text{Re}T_L$	$\text{Im}T_L$
copper $a_0 = 6.8087$ a. u. $E_F = 0.55$ Ry	0 Γ_1	0.0755	0.5591	0.0761	0.0032	-0.4508	-0.0918
	1 Γ_{15}	0.1298	0.8310	0.1241	0.0139	-0.1075	0.2959
	2 Γ_{12}	-0.1186	1.0732	-0.1323	0.0150	-0.1530	0.9319
	2 $\Gamma_{25'}$	-0.1186	1.1171	-0.1286	0.0156	-0.0686	0.7312
silver $a_0 = 7.6897$ a. u. $E_F = 0.41$ Ry	0 Γ_1	0.2097	0.6173	0.2150	0.0267	-0.4301	-0.1183
	1 Γ_{15}	0.1188	0.8449	0.1139	0.0119	-0.0954	0.3059
	2 Γ_{12}	-0.1019	1.0618	-0.1124	0.0110	-0.1381	0.9645
	2 $\Gamma_{25'}$	-0.1019	1.1798	-0.1098	0.0122	0.0004	0.7825
gold $a_0 = 7.6821$ a. u. $E_F = 0.41$ Ry	0 Γ_1	0.5395	0.6623	0.6772	0.1748	-0.6426	-0.2855
	1 Γ_{15}	0.1854	0.5097	0.1695	0.0173	-0.4031	0.5083
	2 Γ_{12}	-0.1518	1.2528	-0.1933	0.0287	-0.2498	1.4748
	2 $\Gamma_{25'}$	-0.1518	1.7723	-0.1850	0.0405	0.1296	1.3796
gold $a_0 = 7.6821$ a. u. $E_F = 0.53$ Ry	0 Γ_1	0.2496	0.6829	0.2917	0.0417	-0.5197	-0.5633
	1 Γ_{15}	0.0632	0.5273	0.0622	0.0021	-0.4578	0.2572
	2 Γ_{12}	-0.2426	0.8994	-0.3149	0.0519	-0.4905	0.9492
	2 $\Gamma_{25'}$	-0.2426	1.2752	-0.3040	0.0736	-0.2477	0.9335

anisotropies in this way.

In Ref. 15, experimental Dingle-temperature anisotropies were analyzed to yield a set of three scattering parameters, neglecting the distinction between the two d -like representations Γ_{12} and $\Gamma_{25'}$, and we should investigate the accuracy of this approximation. Let us write the d -wave contribution to the inverse relaxation time in terms of the quantities

$$t_{\frac{1}{2}}^{\pm} = t_{\frac{1}{2}}^{\Gamma_{12}} \pm t_{\frac{1}{2}}^{\Gamma_{25'}}, \quad (36)$$

$$S^* = \frac{1}{2}(S_{\Gamma_{12}} \pm S_{\Gamma_{25'}}).$$

Then the d -wave contribution to Eq. (16) takes the form

$$1/\tau_d(\vec{k}) = (2c/\hbar)(t_{\frac{1}{2}}^+ \text{Im}S^+ + t_{\frac{1}{2}}^- \text{Im}S^-). \quad (37)$$

Neglecting the distinction between the two d representations is equivalent to assuming

$$t_{\frac{1}{2}}^+ \text{Im}S^+ \gg t_{\frac{1}{2}}^- \text{Im}S^-. \quad (38)$$

Typically $t_{\frac{1}{2}}^+$ is of order 20% of $t_{\frac{1}{2}}^-$, so it can be seen that the condition is satisfied to within a few percent, i.e., comparable with experimental errors, if

$$\text{Im}(S_{\Gamma_{12}} + S_{\Gamma_{25'}}) \gg 0.2 \text{Im}(S_{\Gamma_{12}} - S_{\Gamma_{25'}}). \quad (39)$$

The values in Table III show that this condition is satisfied rather well for copper and silver, and even in gold the maximum correction to the expression for the Dingle temperature is only of order 3%. The error which occurs if the difference between the two representations is neglected when calculating $\text{Re}S_L$ from the Fermi-surface changes is an order of magnitude smaller.

It is straightforward to interpret $\text{Im}S_L$ (or equivalently the Friedel phase shifts) to give impurity state parameters. We note from Eq. (33) that there are two values of ξ_i consistent with a given experimental value of $\text{Im}S_L$. This ambiguity is related to the fact that the signs of the Friedel phase shifts cannot be determined from scattering anisotropies. By evaluating the displaced charge in the vicinity of the impurity atom^{15,22} it has been shown that the Friedel phase shifts are given by

$$\tan\phi_L = \text{Im}\chi_L / (\xi_i - \text{Re}\chi_L). \quad (40)$$

Thus, when the sign of ϕ_L can be determined from other considerations (see Ref. 15), the values of ξ_i can also be uniquely determined.

When analyzing impurity-induced changes in the

TABLE III. Summary of scattering parameters derived from Dingle-temperature data. The errors are derived as explained in Ref. 15. Fits to the Dingle-temperature data have been constrained to give the correct residual resistivity, and signs have been determined as described in the text.

	$\text{Im}S_0$	$\text{Im}S_1$	$\text{Im}S_{\Gamma_{12}}$	$\text{Im}S_{\Gamma_{25'}}$	ϕ_0	ϕ_1	$\phi_{\Gamma_{12}}$	$\phi_{\Gamma_{25'}}$	\mathcal{F}
Cu(Ni) ^a	0.0(2)	0.0045(30)	0.062(30)	0.063(30)	0.0(2)	-0.061(35)	-0.26(6)	-0.27(6)	-0.96
Cu(Ge) ^a	0.02(50)	0.54(15)	0.042(50)	0.044(50)	0.09(50)	0.73(15)	0.21(25)	0.22(25)	2.14
Cu(Au) ^a	0.07(15)	0.013(10)	0.016(10)	0.016(10)	0.20(15)	-0.10(5)	-0.13(8)	-0.13(8)	-0.48
Ag(Au) ^b	0.057(3)	0.0092(2)	0.0055(10)	0.0057(10)	0.19(1)	0.088(2)	-0.076(6)	-0.082(6)	0.04
Ag(Sn) ^b	0.08(7)	0.60(2)	0.04(1)	0.04(1)	0.23(20)	0.80(2)	0.20(15)	0.22(15)	2.35
Au(Ag) ^c	0.10(6)	0.009(7)	0.0013(6)	0.0019(6)	-0.26(7)	-0.067(25)	0.04(6)	0.06(6)	-0.13
Au(Cu) ^c	0.06(4)	0.011(7)	0.006(5)	0.008(5)	-0.20(6)	0.075(20)	0.084(30)	0.12(3)	0.35
Au(Ga) ^c	1.10(8)	0.312(70)	0.011(6)	0.016(6)	0.98(6)	0.41(5)	0.12(3)	0.18(3)	1.90

^aReference 2.^bReference 3.^cReference 4.^dReference 33.

TABLE IV. Summary of scattering parameters derived from impurity-induced Fermi-surface changes.

	$\text{Re}S_0$	$\text{Re}S_1$	$\text{Re}S_{\Gamma_1}$	$\text{Re}S_{\Gamma_{25'}}$	ϕ_0	ϕ_1	$\phi_{\Gamma_{12}}$	$\phi_{\Gamma_{25'}}$	\mathfrak{F}
Cu(Al) ^a	0.37(25)	0.489(30)	0.24(4)	0.26(4)	0.22(20)	0.481(30)	0.27(4)	0.30(4)	1.99
Cu(Ni) ^a	-0.46(40)	-0.063(40)	-0.22(6)	-0.20(6)	-0.27(20)	-0.053(40)	-0.24(7)	-0.24(7)	-1.04
Ag(Au) ^b	0.216(60)	0.037(5)	-0.044(8)	-0.043(8)	0.135(40)	0.032(4)	-0.047(10)	-0.051(10)	-0.01
Au(Ag)	-0.33(10)	-0.08(1)	0.043(10)	0.044(10)	-0.22(7)	-0.047(8)	0.054(10)	0.077(10)	0.09

^aReference 10.^bReference 32.

Fermi radius to yield $\text{Re}S_L$ an exactly parallel analysis is possible. Corresponding to Eq. (33) we find

$$\text{Re}S_L = \sin^2 \eta_i^h \frac{\xi_l - \text{Re}\chi_L}{(\xi_l - \text{Re}\chi_L)^2 + (\text{Im}\chi_L)^2}, \quad (41)$$

so again for $l \leq 2$ the data can be analyzed to yield the three parameters ξ_l . The results of such analyses are summarized in Table IV. Note that the signs of the Friedel phase shifts are determined by the Fermi-surface changes, so in this case there is no ambiguity in ξ_l .

An explicit expression for the impurity phase shifts in terms of the Friedel phase shifts can be obtained by combining Eqs. (33) and (40):

$$\cot \eta_i^f = \cot \eta_i^h - (\text{Re}\chi_L + \cot \phi_L \text{Im}\chi_L)^{-1}. \quad (42)$$

The magnitude of the renormalization coefficient $|\alpha_L|$ is then conveniently given by $\sin \phi_L / I_L \sin \Delta \eta_i$ (Eq. 24), and its phase by

$$\theta_L = \phi_L - \Delta \eta_i. \quad (43)$$

Thus the impurity scattering phase shifts η_i^f , and the complex renormalization coefficients α_L , evaluated at the Fermi energy of the host metal, can be determined unambiguously provided that the magnitudes and signs of the Friedel phase shifts are known. Results for the impurity phase shifts will be presented in Sec. IV C.

The preceding analysis is based on a muffin-tin approximation for the host and impurity potentials. If there are significant nonspherical components of the potentials that are confined within the muffin-tin spheres, this analysis can be extended by allowing the phase shifts to depend on the point-group representation. For partial waves $l \leq 2$ and cubic point symmetry this means taking two independent d -wave phase shifts. However, corrections due to nonspherical components of the potential outside the muffin-tin sphere cannot be handled by simple extension of the present analysis.

C. Approximation for back scattering

Although, as outlined above, it is possible to evaluate the back scattering exactly within the muffin-tin approximation, it is of interest to consider various approximate treatments. We know from the discussion above that it is invalid to neglect back scattering completely. The back scattering matrix T_r depends upon both the real and imaginary

parts of the Brillouin-zone integral χ , Eq. (27). The imaginary part of χ_L^r (or I_L) is an integral over the Fermi surface and is easily evaluated. On the other hand, the real part of χ involves a principal-parts integral throughout the volume of the Brillouin zone. The following approximations enable one to estimate T_L without having to evaluate the volume Brillouin-zone integrals. In the following discussion we will assume the scattering for f and higher partial waves can be neglected, in which case the diagonal representation for α_L and T_L is valid.

Combining Eqs. (13), (15), and (21), we find that in order to satisfy the optical theorem T_L must lie on a circle in the complex T plane, whose center is $X + iY$ where

$$X = [(2I_L \sin^2 \eta_i^h)^{-1} - 1], \quad (44)$$

$$Y = -\cot \eta_i^h, \quad (45)$$

and whose radius is

$$R = X + 1. \quad (46)$$

For a free-electron host $I_L = 1$, $\eta_i^f = 0$, and the circle reduces to a straight line through the origin ($T_L = 0$). For a real metal the circle has a large radius, as shown in Fig. 1 in the case of copper. Comparison with the free-electron limit suggested the "minimum scattering" criterion for estimating the back scattering. This is the assumption¹⁷ that the back scattering coefficients lie on the circle at the point closest to the origin. Back scattering coefficients for copper estimated from the minimum scattering criterion are shown in Fig. 2. Also shown are the exact values of T_L taken from Table II. It will be seen that the criterion predicts results of the correct magnitude. The values of $|\alpha_L|$

TABLE V. Impurity phase shifts (radians) calculated from impurity potentials constructed as described in the text. They correspond to the Fermi-energy parameter $E_F = 0.55$ Ry, which has been assumed in the analysis of copper-based alloys. Also listed is the assumed electronic configuration of the impurity atom.

Config.	η_0^f	η_1^f	η_2^f
Cu(Ni) $3d^9 4s^1$	-0.198	-0.033	-0.299
Cu(Zn) $4s^2$	0.569	0.397	0.009
Cu(Ga) $4s^2 4p^1$	0.965	0.868	0.033
Cu(Ge) $4s^2 4p^2$	1.209	1.388	0.052
Cu(Al) $3s^2 3p^1$	0.817	0.894	0.073

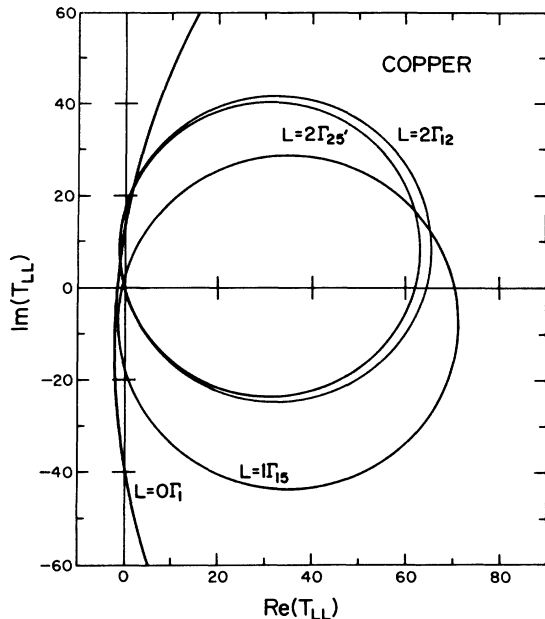


FIG. 1. The scattering circles are the loci of back scattering coefficients constrained to satisfy the optical theorem for a copper lattice.

and θ_L (see Table IV) are in fair agreement with the correct values for s - and p -wave scattering, but agreement for d waves is less satisfactory.

Two alternative expressions have been found to give approximately correct values of the back scattering in the noble metals. The first is to take $\text{Re}T_L = I_L = 1$ and to adjust $\text{Im}T_L$ so that T_L lies on the scattering circle. The second is to take $\text{Re}\chi_L = \tan\eta_L^h$, to evaluate $\text{Im}\chi_L$ from Eq. (29), and to calculate T_L from Eq. (30). The values of T_L obtained in these approximations are plotted in Fig. 2. It will be seen that they yield results very similar to those of the minimum scattering approximation. The various approximate treatments of back scattering are most accurate for weak scattering, so they might be expected to be adequate for simple metal hosts. Our results suggest, however, that they break down near a resonance of the host or the impurity resonance as, for example, occurs for d -wave scattering in the noble metals or with impurities which show strong p -wave scattering. In such systems it is necessary to go back to the exact calculation of the χ coefficients in order to analyze the experimental data.

IV. RESULTS AND DISCUSSION

A. Theoretical estimates of impurity phase shifts

It is well known that the scattering phase shifts for electrons at the Fermi level of a pure metal can be determined by analysis of the radial anisotropy of the Fermi surface. The values of the phase

shifts obtained in this way depend strongly on the choice of the Fermi-energy parameter E_F . The quality of the fit is found to be essentially independent of this parameter. However, different values of E_F result from different ways of constructing the crystal potential in the solid, and only a narrow range of values of E_F is likely to yield charge distributions that are accurate within the interstitial region. Physically reasonable values of E_F are perhaps best determined from the results of self-consistent band-structure calculations.

The same problem of determining the Fermi-energy parameter arises in analyzing the alloy data. This is because the coefficients t_k^L show approximately the same anisotropy at different values of the Fermi energy parameter. It follows that the scattering parameters S_L and the Friedel phase shifts ϕ_L are similarly independent of E_F . However, the impurity-state parameters η_i^h and α_L do depend somewhat on the choice of E_F , and for the analysis of experimental data we have selected values of E_F close to those obtained from accurate first-principles calculations for the host metals.

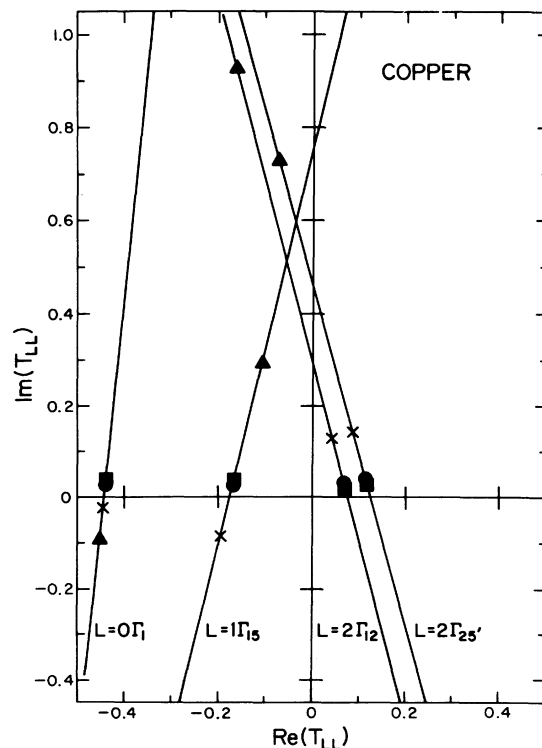


FIG. 2. On the scale of this figure the arcs of the scattering circles are approximately straight lines. The solid triangles \blacktriangle are the back scattering coefficients deduced in the exact calculation. The squares \blacksquare are those obtained in the minimum scattering approximation, the circles \bullet are those obtained in the approximation $\text{Re}T = I_L - 1$, and the crosses \times follow from the approximation $\text{Re}T = \tan \eta_L$.

Because the muffin-tin potential that describes scattering by a given atomic species is expected to depend only weakly on its environment, it seems reasonable to compare the scattering phase shifts for noble-metal impurities in noble-metal hosts with the differences between the phase shifts of the pure metals, provided that both sets of phase shifts correspond to the same value of E_F and that both metals have similar lattice constants. Phase-shift analyses have been carried out for the pure metals copper, silver, gold, and tin, and preliminary work in under way for aluminum. The results of these analyses will be used in interpreting the alloy data for Cu(Au), Ag(Au), Ag(Sn), Au(Cu), Au(Ag), and Cu(Al).

As a guide to the interpretation of the experimental data for other alloys, we have constructed impurity potentials for a series of substitutional impurities in a copper lattice. Impurity potentials for Ni, Zn, Ga, and Ge in copper were obtained by superposition of atomic potentials derived from the self-consistent analytic wave functions due to Bagus, Gilbert, and Roothaan,²³ neglecting any possible impurity-induced distortion of the lattice. Exchange was treated in the Slater²⁴ free-electron approximation. As a check on the procedure it was verified that the "copper in copper" potential yielded phase shifts in satisfactory agreement with experiment. In order to allow for redistribution of charge associated with the screening of the impurity, which cannot be described by the superposition of neutral atom potentials, a small constant shift was added to the potential within the impurity sphere. The shift was adjusted to bring the Friedel sum of the Friedel phase shifts calculated from Eqs. (34) and (42), into agreement with the valence difference according to Eq. (22). The impurity phase shifts calculated in this way for Cu(Ni), Cu(Zn), Cu(Ga), Cu(Ge), and Cu(Al) are presented in Table V. It is emphasized that these results are based on an approximate potential and can do no more than assist in the interpretation of trends within the experimental data.

B. Lattice distortion on alloying

In nearly all cases of alloying there is a change of lattice constant associated with the different atomic sizes of host and impurity atoms. Although the atomic displacements are localized around the impurity site, falling off as $1/r^2$, Eshelby²⁵ has shown that, for a large number of defects scattered uniformly throughout a specimen, there is a uniform expansion with the average lattice constant equal to that measured by x rays. In addition there is a short-range distortion round the impurity site which will cause scattering of the Bloch electrons. Blatt²⁶ and Harrison²⁷ argue that this localized distortion removes to infinity a fraction of the charge around the impurity, so the effective valence differ-

ence between the impurity and the host must be modified by an amount proportional to the lattice distortion.

The uniform distortion modifies the interpretation of Fermi-surface changes because it causes a uniform contraction of the Brillouin zone and a shift of the Fermi energy. The uniform change in lattice constant is allowed for by scaling the raw experimental Fermi-surface areas to correspond to a lattice constant of the alloy equal to that of the pure host (i. e., effectively applying pressure to the alloy). The analysis of the data then proceeds as described above.

The uniform distortion does not affect the scattering data (e. g., applying pressure to a metal does not cause extra scattering). However, the Dingle temperatures presumably include scattering due to the localized distortion around the impurity site, and there seems to be no reliable way to correct for this. The Friedel phase shifts, and other quantities deduced from them, therefore will differ by an amount proportional to the lattice distortion, depending on whether they are deduced from Fermi surface measurements or from the scattering measurements.

We believe that the phase shifts derived from impurity-induced Fermi-surface changes are likely to be the more accurate in that they include a correction for the uniform expansion, and because the anisotropy of the Fermi surface is relatively unaffected by the localized distortion. The localized distortion can be considered as (i) producing a modified $\Delta\eta'_i$, i. e., producing extra scattering, and (ii) modifying the back scattering. The modified back scattering factor α'_L can be written

$$\alpha'_L = |\alpha'_L| \exp[i(\theta_L + \beta_L)], \quad (47)$$

where $|\alpha'_L| \approx |\alpha_L|$ and β_L is the extra phase shift in the back scattering added by the lattice distortion. The measured scattering parameters S'_L are then given by

$$S'_L = |\alpha'_L| \sin\Delta\eta'_i \exp[i(\Delta\eta'_i + \theta_L + \beta_L)] \quad (48)$$

or approximately

$$S'_L \approx I_L^{-1} \sin\phi_L \exp[i(\phi_L + \beta_L)]. \quad (49)$$

In all alloy systems considered here ϕ_L is relatively small ($< \frac{1}{4}\pi$), and β_L will presumably be of comparable size. It is then a fair approximation to write $\cos(\phi_L + \beta_L) \approx 1$ and ϕ_L can be deduced from $\text{Re}S'_L$ with a fair degree of accuracy. The Friedel phase shifts ϕ_L^{scatt} derived from the scattering parameters by writing

$$\begin{aligned} \text{Im}S'_L &= I_L^{-1} \sin\phi_L \sin(\phi_L + \beta_L) \\ &\equiv I_L^{-1} \sin^2\phi_L^{\text{scatt}} \end{aligned} \quad (50)$$

may, however, deviate from the correct values ϕ_L by an amount of order β_L which is comparable to ϕ_L .

This conclusion is supported by the experimental evidence that Friedel sums determined from ReS_L agree rather well with the valence difference between host and impurity, whereas those determined from scattering data frequently disagree markedly (by up to 50%). Furthermore, the disagreement appears to correlate strongly with the existence of large lattice distortions, the discrepancy being small for $\text{Cu}(\text{Ni})$ and $\text{Au}(\text{Ga})$ where the distortion is small. Whether or not this argument proves to be correct, it should be emphasized that the phase shifts deduced from Fermi-surface changes are essentially different from those determined in scattering experiments.

C. Detailed comparisons

1. Ag-Au system

In this system both Fermi-surface and scattering results are available for both dilute alloys. We compare below the measured values of $\Delta\eta_l$ with the values $\Delta\eta_l^{\text{pure}}$ derived from phase-shift parametrizations of the pure metals. The quoted errors are the random errors in the fit estimated according to the procedure in Ref. 10, and in this case all results are obtained with $E_F = 0.41$ Ry.

Ag(Au)	l	$\Delta\eta_l^{\text{scatt}}$	$\Delta\eta_l^{\text{FS}}$	$\Delta\eta_l^{\text{pure}}$
	0	0.279(20)	0.205(60)	0.330
	1	0.107(3)	0.038(5)	0.067
	2	-0.066(5)	-0.042(10)	-0.050
Au(Ag)	0	-0.555(150)	-0.450(150)	-0.330
	1	-0.125(50)	-0.088(15)	-0.067
	2	0.035(40)	0.047(10)	+0.050

The agreement is generally quite acceptable, although the Fermi-surface results are systematically smaller in magnitude than the scattering results. Although the lattice distortion is very small

($\sim -0.01\%$ /at. % for both alloys), the correction to the Fermi-surface results is comparable to the measured changes because the scattering potential is weak. It is therefore not unreasonable to attribute the discrepancy to lattice distortion. Alternatively, the discrepancy might be associated with systematic errors in determining the concentrations in the two experiments. It is gratifying to note that the pure metal phase shifts generally give a rather good estimate of the Fermi-surface changes on alloying.

There has been some discussion of the problem of charge flow in this system. The Mössbauer isomer shifts²⁸ suggest a flow of s -like charge onto the gold sites, and photoelectron spectroscopy results²⁹ have been interpreted to mean that the s charge flow is compensated by a reverse flow of d charge. In contrast, Levin and Ehrenreich,³⁰ comparing a coherent-potential-approximation model calculation with optical experiments, find best agreement when there is a flow of s -like charge from gold atoms to silver atoms. Taken at face value our results agree with the former suggestion. The signs of the s and d phase shifts suggest an excess of s charge on the Au atoms and an excess of d charge on the Ag atoms.

2. Cu-Au system

In this system only scattering results are at present available. Because the lattice constants of the two metals are markedly different ($\sim 11\%$), we might expect the phase shifts to include large lattice distortion effects. In comparing the scattering phase shifts with those deduced from pure metal parametrizations, we should again use the same values of E_F for impurity and host. The gold calculations were carried out at 0.41 and 0.53 Ry and a small correction was applied to correspond to $E_F = 0.55$ Ry. Again the quoted errors do not allow for possible systematic errors.

			$l = 0$	1	2	
Cu(Au)	0.55	Ry	$\Delta\eta_l^{\text{scatt}}$	0.33(25)	-0.12(6)	-0.11(7)
			$\Delta\eta_l^{\text{pure}}$	0.13	-0.09	-0.14
Au(Cu)	0.55	Ry	$\Delta\eta_l^{\text{scatt}}$	-0.38(11)	0.14(4)	0.11(3)
			$\Delta\eta_l^{\text{pure}}$	-0.13	0.09	0.13
Au(Cu)	0.41	Ry	$\Delta\eta_l^{\text{scatt}}$	-0.40(11)	0.15 ₄ (4)	0.08(2)
			$\Delta\eta_l^{\text{pure}}$	-0.23	0.01 ₈	0.09 ₃

The two sets of phase shifts are similar in magnitude, and their signs suggest a charge flow in the sense as Ag-Au, i. e., flow of s charge onto the Au atoms compensated by a reverse flow of d charge. The gold results show that the scattering phase shifts

are relatively independent of the choice of E_F .

3. Ag(Sn)

This is another alloy in which there are in the literature both experimental data and phase-shift

analyses of the two constituents. The scattering data show decisively the predominance of p -wave scattering. In the phase-shift analysis of the Fermi-surface data for white tin, Devillers and de Vroomen³¹ express their results as logarithmic derivatives of the radial wave function at the muffin-tin radius. This can readily be expressed in terms of phase shifts at the value of Fermi-energy parameter used in the silver alloy analysis, $E_F = 0.41$. Comparing the sets of phase shifts:

l	$\Delta\eta_l^{\text{scatt}}$	$\Delta\eta_l^{\text{pure}}$
0	0.33(30)	0.71
1	1.06(3)	0.79
2	0.23(20)	0.09

In this system we expect the results will be affected by lattice distortion (0.05%/at. %). In fact, the discrepancy is in the opposite sense to those noted above. The general dominance of the p -wave term is certainly reproduced, but because the coordination in white tin is much lower than that of a substitutional site in silver, comparison between the two sets of phase shifts can be little more than qualitative. Taken at their face value, however, they suggest the charge density is enhanced at the center of the impurity cell in the alloy over that in the pure metal.

4. Cu(Al)

In this system, Fermi-surface results are available, and there is also a preliminary phase-shift parametrization of pure aluminum.³² Lattice distortion is present but not gross (0.07%/at. %). We compare the various phase shifts together with those calculated theoretically according to the prescription given in Sec. IV A. All results are at $E_F = 0.55$ Ry.

l	$\Delta\eta_l^{\text{FS}}$	$\Delta\eta_l^{\text{pure}}$	$\Delta\eta_l^{\text{calc}}$
0	0.36(3)	0.49	0.753
1	0.64(4)	0.41	0.768
2	0.36(5)	0.17	0.190

In this case the agreement is rather poor. It may be that the anomalously large d phase shift determined from the Fermi-surface results is associated with experimental errors. If this is so, reducing the d phase shift should be reflected in an increased s phase shift, bringing better agreement with the calculated values. The values derived from the host parametrizations, although showing the correct trend, are also in disagreement with the experimental results.

5. Cu(Ni)

In this system both Fermi-surface and scattering

data are available and lattice distortion is small (-0.03% /at. %). We compare below the measured phase shifts with values calculated in Sec. IV A.

l	$\Delta\eta_l^{\text{scatt}}$	$\Delta\eta_l^{\text{FS}}$	$\Delta\eta_l^{\text{calc}}$
0	0.0(3)	-0.50(4)	-0.27
1	-0.07(4)	-0.06(4)	-0.09 ₇
2	-0.20(5)	-0.18(5)	-0.18 ₁

In this case there is rather good agreement between both the sets of measured phase shifts and the calculated values and all results show a large d phase shift characteristic of the nickel d resonance or virtual bound state. There is apparently a small residual lattice distortion effect reflected mainly in the s phase shift. The generally good agreement gives some confidence that, in the absence of lattice distortion, the calculated impurity potentials approximate the correct impurity potentials.

6. Cu(Ge)

In this alloy the lattice distortion is large (0.1%/at. %) and only scattering results are available. These are dominated by the p phase shift, and there are large uncertainties in the s and d phase shifts. We compare the results with the calculated values.

l	$\Delta\eta_l^{\text{scatt}}$	$\Delta\eta_l^{\text{calc}}$
0	0.17(100)	1.15
1	0.98(19)	1.26
2	0.24(30)	0.17

Given the large uncertainties in the s and d phase shifts, the agreement is acceptable. Again, the results suggest a reduction of the s phase shift and an enhancement of the d phase shift which is in the same sense as the Cu(Ni) and which may reflect lattice distortion effects.

7. Au(Ga)

This system is characterized by a very small lattice distortion (0.015%/at. %) but, unlike the Au(Ag) system, there is a large potential difference. Only Dingle-temperature results for two orbits are available.³³ A simple analysis based on the data of Ref. 33, and the residual resistivity (2.15 $\mu\Omega$ cm/at. %), yields the following results for $E_F = 0.41$ Ry:

l	$\Delta\eta_l^{\text{scatt}}$
0	0.63(4)
1	0.88(11)
2	0.12(3)

Unfortunately, no theoretical estimates are available for comparison. This simple analysis appears to

be consistent with a more complete analysis based on Dingle-temperature data for 6 orbits, which is to be published.³⁴ It is gratifying to note that, unlike alloys where the lattice distortion is large, the Friedel sum is rather close to the valence difference of 2.

V. CONCLUSIONS

In dilute alloys, Friedel phase shifts can be determined experimentally either from the anisotropy of the changes in de Haas-van Alphen frequency on alloying, or from the anisotropy of Dingle temperatures. We have shown how these experimental phase shifts can be separated into a contribution from the impurity potential and a contribution from back scattering by the host lattice. The latter can be calculated exactly, within the muffin-tin approximation, but this requires a Brillouin-zone integration. It is *always* inconsistent to neglect back scattering completely when analyzing the anisotropy of experimental data. However, we have found several approximations to back scattering which prove satisfactory in special cases, notably far from scattering resonances.

When back scattering is included, experimental estimates can be obtained for the phase shifts that characterize the impurity in the host. These phase

shifts are expected to include a contribution from any lattice distortion present, but this contribution depends on the type of measurement.

Experimentally, such differences are found when Fermi surface and scattering data are compared. In systems where lattice distortion is small, the phase shifts ϕ^{FS} and ϕ^{scatt} , are generally in agreement, and the scattering results yield the correct value of the Friedel sum. When lattice distortion is appreciable ϕ^{FS} may no longer equal ϕ^{scatt} , but the Fermi-surface results appear always to give the correct Friedel sum.

The experimental phase shifts in copper alloys are in generally satisfactory agreement with those calculated from a potential generated by a superposition of atomic wave functions. In the homovalent noble-metal alloys it is found that even when the lattice distortion is large, as it is in Cu-Au, the differences between the phase shifts derived from analyses of Fermi-surface distortions of the pure metals provide a fair approximation to the scattering phase shifts.

ACKNOWLEDGMENTS

We are indebted to Professor D. H. Lowndes and Dr. I. M. Templeton for communicating to us certain of their results prior to publication.

*Present address: Dept. of Metallurgy and Materials Science, University of Pennsylvania, Philadelphia, Penn. 19174.

¹For a review see M. Springford, *Adv. Phys.* **20**, 493 (1971).

²R. G. Poulsen, D. L. Randles, and M. Springford, *J. Phys. F* **4**, 981 (1974).

³H. R. Brown and A. Myers, *J. Phys. F* **2**, 683 (1972); and revised results (private communication).

⁴D. H. Lowndes, K. M. Miller, R. G. Poulsen, and M. Springford, *Proc. R. Soc. Lond. A* **331**, 497 (1973).

⁵G. J. Morgan, *Proc. Phys. Soc. Lond.* **89**, 365 (1966).

⁶J. W. Blaker and R. Harris, *J. Phys. C* **4**, 569 (1971).

⁷P. T. Coleridge, *J. Phys. F* **2**, 1016 (1972).

⁸P. T. Coleridge, *Phys. Rev.* **7**, 3508 (1973).

⁹R. Harris and B. G. Mulimani, *J. Phys. F* **4**, 403 (1974).

¹⁰I. M. Templeton and P. T. Coleridge, *J. Phys. F* **5**, 1307 (1975).

¹¹P. T. Coleridge, *J. Phys. F* **5**, 1317 (1975).

¹²J. B. Boyce and C. P. Slichter, *Phys. Rev. Lett.* **32**, 61 (1974).

¹³J. Winter, *Magnetic Resonance in Metals* (Clarendon, Oxford, 1971), Chap. 10 and references therein.

¹⁴W. Kohn and N. Rostoker, *Phys. Rev.* **94**, 1111 (1954).

¹⁵P. T. Coleridge, N. A. W. Holzwarth, and M. J. G. Lee, *Phys. Rev.* **10**, 1213 (1974).

¹⁶N. A. W. Holzwarth, *Phys. Rev. B* **11**, 3718 (1975).

¹⁷P. T. Coleridge and M. J. G. Lee, *Phys. Rev. Lett.*

31, 997 (1973).

¹⁸J. Friedel, *Philos. Mag.* **43**, 153 (1952).

¹⁹E. A. Stern, *Phys. Rev.* **168**, 730 (1968).

²⁰T. H. Dupree, *Ann. Phys. (N.Y.)* **15**, 63 (1961).

²¹F. B. Hildebrand, *Advanced Calculus for Applications* (Prentice-Hall, Englewood Cliffs, 1962), Chap. 10.

²²R. H. Lasseter and P. Soven, *Phys. Rev. B* **8**, 2476 (1973).

²³P. S. Bagus, T. L. Gilbert, and C. C. J. Roothan, Argonne National Lab. Report, 1972 (unpublished).

²⁴J. C. Slater, *Phys. Rev.* **81**, 385 (1951).

²⁵J. D. Eshelby, *J. Appl. Phys.* **25**, 255 (1954).

²⁶F. J. Blatt, *Phys. Rev.* **108**, 285 (1957).

²⁷W. A. Harrison, *Phys. Rev.* **110**, 14 (1958).

²⁸See, e.g., R. L. Cohen, Y. Yafet, and K. W. West, *Phys. Rev. B* **3**, 2872 (1971).

²⁹R. E. Watson, J. Hudis, and M. L. Perlman, *Phys. Rev. B* **4**, 4139 (1971).

³⁰K. Levin and H. Ehrenreich, *Phys. Rev. B* **3**, 4172 (1971).

³¹M. A. C. Devillers and A. R. de Vroomen, *Phys. Lett. A* **30**, 159 (1969).

³²P. T. Coleridge (unpublished).

³³D. H. Dye, D. H. Lowndes, G. W. Crabtree, L. R. Windmiller, and J. B. Ketterson, *Bull. Am. Phys. Soc.* **20**, 353 (1975).

³⁴D. H. Lowndes (private communication).